

Recognizing Emotions Induced by Affective Sounds through Heart Rate Variability

Mimma Nardelli, Gaetano Valenza*, Member, IEEE, Alberto Greco, Antonio Lanata, Member, IEEE, and Enzo Pasquale Scilingo, Member, IEEE

Abstract—This paper reports on how emotional states elicited by affective sounds can be effectively recognized by means of estimates of Autonomic Nervous System (ANS) dynamics. Specifically, emotional states are modeled as a combination of arousal and valence dimensions according to the well-known circumplex model of affect, whereas the ANS dynamics is estimated through standard and nonlinear analysis of Heart rate variability (HRV) exclusively, which is derived from the electrocardiogram (ECG). In addition, Lagged Poincaré Plots of the HRV series were also taken into account. The affective sounds were gathered from the International Affective Digitized Sound System and grouped into four different levels of arousal (intensity) and two levels of valence (unpleasant and pleasant). A group of 27 healthy volunteers were administered with these standardized stimuli while ECG signals were continuously recorded. Then, those HRV features showing significant changes ($p < 0.05$ from statistical tests) between the arousal and valence dimensions were used as input of an automatic classification system for the recognition of the four classes of arousal and two classes of valence. Experimental results demonstrated that a quadratic discriminant classifier, tested through Leave-One-Subject-Out procedure, was able to achieve a recognition accuracy of 84.72% on the valence dimension, and 84.26% on the arousal dimension.

Index Terms—Emotion Recognition, Heart rate variability, Autonomic Nervous System, Nonlinear Analysis, Poincaré plot, Affective Digitized Sound System (IADS), Quadratic Discriminant Classifier.

1 INTRODUCTION

THE automatic quantification and recognition of human emotions is a relatively new and fast-growing research area which combines knowledge in the fields of psychophysiology, computer science, biomedical engineering, and artificial intelligence. Results of these studies are usually identified within the so-called "Affective Computing" field, providing computational models and machine learning algorithms for the automatic recognition of emotional regulation occurring through different kinds of elicitation [1]. In general, an emotion recognition system is designed to be effective for a specific kind of stimulus and it is built on a specific model of emotion which has to be characterized by processing one or more physiological/behavioral signs.

In this study, the Russel's Circumplex model of affect [2], [3], which is one of mostly used model of emotions, is used to model emotions elicited by affective sounds. More specifically, considering such a model, each emotion is seen as a linear combination of two affective dimensions: arousal and valence. The arousal dimension expresses the intensity of the emotion, whereas the valence dimension quantifies how much positive or negative an emotion is felt by the subject along a continuum of pleasantness-unpleasantness (Figure 1).

Concerning the physiological signals to be taken into account for emotion recognition, ECG-derived series, which mainly refer to the analysis of Heart Rate Variability (HRV),

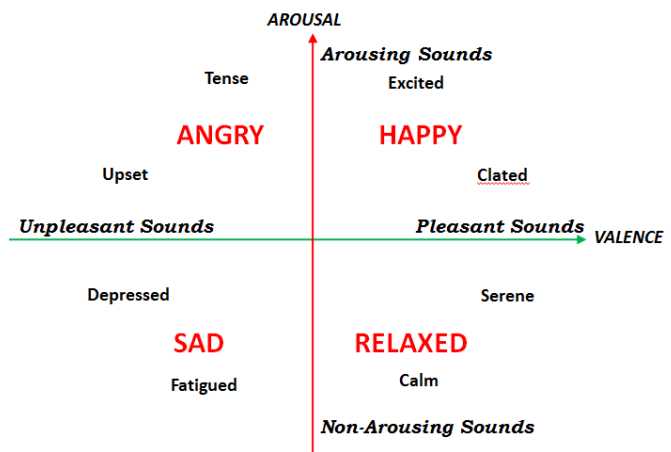


Figure 1: A graphical representation of Russell's circumplex model of emotions for acoustic stimuli: the horizontal axis represents the valence dimension and the vertical axis represents the arousal dimension.

have been extensively proposed in the literature along with other Autonomic Nervous System (ANS)-derived signals such as diastolic and systolic blood pressure, pupillary dilatation, respiration, temperature and skin conductance [4]–[18].

Although the majority of the affective computing studies, based on ANS dynamics, includes the analysis of several time series, in this study we propose an effective emotion recognition system based on measures derived from the HRV exclusively.

Also regarding the emotion elicitation, a wide range of

* Corresponding Author.

The authors are with the Department of Information Engineering & Research Centre E. Piaggio, School of Engineering, University of Pisa, Pisa, Italy

elicitation methods have been proposed in the literature: real experiences [19], film clips [16], [20]–[22], problem solving [23], computer game interfaces [24], images [9], [25], as spoken words [26] and music [27]–[29]. The computational system proposed in this study is developed to recognize emotions through the identification of the elicited arousal and valence levels of standardized acoustic stimuli gathered from the International Affective Digitized Sound system (IADS) [30]. Likewise the IAPS database [31], [32], IADS is a database of affective sounds characterized in terms of valence and arousal dimensions [30]. Of note, the use of standardized stimuli allows replicating studies in a more reliable fashion, making also easier the comparison of the results with future works.

In this work, we first provide a comprehensive characterization of the heartbeat dynamics upon the administration of IADS affective stimuli having different levels of arousal and valence, including the neutral one. Such a characterization is performed deriving standard measures, which are defined in the time and frequency domain, from the HRV as recommended by the current guidelines [33], and nonlinear measures, which are defined in the phase space domain. This choice is strongly motivated by the intrinsic nonlinear nature of the cardiovascular dynamics which is the result of signaling and nonlinear interactions of the neurotransmitters in the sino-atrial node [34]. Moreover, our previous achievements have highlighted the crucial role of ANS nonlinear dynamics emotion regulation, and arousal and valence recognition [5], [35]–[40]. In this study, features extracted from Poincaré plots were also taken into account. Specifically, we engaged geometric indices of Lagged Poincaré plots (LPP) which have already been successfully proposed in the literature in studies involving acoustic stimulation [41]–[43]. Therefore, we included these features in our set of HRV nonlinear measures. Finally, only those HRV measures showing statistical significant differences between the elicited arousal or valence levels are considered as input of an automatic emotion recognition system based on the Quadratic Discriminant classifier (QDC) [44], [45], which is based on the Bayesian decision theory.

1.1 Previous Studies on Music and Affective Sounds

IADS sounds have been already jointly used to IAPS images to elicit emotions in healthy subjects [46], [47]. In these cases, the subject's physiological response was investigated through HRV series analysis, calculating heart rate (HR) changes and seeking for HR decelerations during the stimuli. It was found that unpleasant audio stimuli induces a higher HR deceleration as compared with visual stimuli [47]. There are few other studies in the literature using IADS sounds [48]–[50] showing changes of facial electromyographic and electroencephalographic (EEG) activity [48], [49].

In the literature there are other several studies dealing with pleasant and unpleasant music and music-induced emotions [27]–[29], [41], [42], [51], [52]. These studies take into account EEG and ANS dynamics, also to automatically recognize four types of music-induced emotions [51]. Of note, during music-induced emotion, a significant parasympathetic modulation occurs [52]. Moreover, the use of functional Magnetic Resonance Imaging (fMRI) allowed to high-

light the role of the amygdala during emotional audiovisual stimuli [53].

2 MATERIALS AND METHODS

2.1 Subjects Recruitment, Experimental protocol and Acquisition set-up

Twenty-seven healthy subjects, aged from 25 to 35, participated as volunteers in the experiment. According to the self-report questionnaires, none of them had a history of injury of the auditory canal or partial or full incapability of hearing. Moreover, none of them suffered from any cardiovascular, mental or chronic disease. Participants were informed about the protocol and about the purpose of the study, but they were not informed about the arousal and valence levels they would have been listened to. During the experiment, participants were seated in a comfortable chair in a controlled environment while listening to the IADS sounds. Each subject was left alone in the room where the experiment took place for the whole duration (29 minutes). The acoustic stimulation was performed by using headphones while the subject's eyes were closed, to avoid any kind of visual interference.

The affective elicitation was comprised of 10 sessions: after an initial resting session of 5 minutes, four arousal sessions alternated with neutral sessions (see Figure 2). The four arousal levels had different increasing scores. Within each arousing session, the acoustic stimuli were selected to have Low-Medium (L-M) for negative valence and Medium-High (M-H) for positive valence. Such levels were set according to the IADS valence and arousal scores reported in table 1. The neutral session had a duration of 1 minute and 28 seconds, while the four arousal sessions had a duration of 3 minutes and 30 seconds, 3 minutes and 40 seconds, 4 minutes, 5 minutes and 20 seconds, respectively. The different duration of each arousal session is due to the different length of acoustic stimuli having the same range of positive and negative valence. This experimental protocol was approved by the local ethical committee.

During the elicitation, the ECG was continuously acquired, following the Einthoven triangle configuration, by means of a dedicate hardware module, i.e. the ECG100C Electrocardiogram Amplifier from BIOPAC inc. with a sampling rate of 500 Hz. The ECG signal was exclusively acquired to extract the HRV series, which refers to the variation of the time intervals between consecutive heartbeats identified with R-waves (RR intervals). Therefore, to obtain the HRV series from the ECG, a QRS complex detection algorithm was used, i.e. the automatic algorithm developed by Pan-Tompkins [54]. This algorithm allowed us to extract each QRS complex and to detect the corresponding R-peak. Hence, the RR interval is defined as the interval between two successive QRS complexes. Nevertheless, not all of the RR intervals obtained by the automatic QRS detection algorithm were correct. Any technical artifact (i.e. errors due to the R-peak detection algorithm) in the RR interval time series may interfere with the analysis of these signals. Therefore, an artifact removal algorithm was used. In this work we adopted a proper piecewise cubic spline interpolation method [55]. Besides the mentioned technical ones, physiological artifacts could be also present in the analyzed

RR series. They include ectopic beats and arrhythmic events. We manually checked for physiological artifacts and only artifact-free sections have been included in the analysis. Another common feature that can significantly alter the analysis is the slow trend within the analyzed RR series. In fact, slow non-stationarities can be present in HRV signals and should be considered before the analysis [56]. In this work, the detrending procedure was implemented by means of an advanced method originally presented in [57]. This approach was based on smoothness priors regularization.

Table 1: Rating of IADS sounds used in this work

| Session | N. of Sounds | Valence Rating | Valence Range | Arousal Rating | Arousal Range |
|-----------|--------------|------------------|-----------------|------------------|-----------------|
| Neutral | 8 | 5.915 ± 0.68 | 4.34 ± 6.44 | 3.47 ± 0.175 | 2.88 ± 3.93 |
| Arousal 1 | 19 | / | 3.54 ± 7.51 | 4.60 ± 0.21 | 4.03 ± 4.97 |
| Arousal 2 | 19 | / | 2.46 ± 7.78 | 5.42 ± 0.22 | 5.00 ± 5.89 |
| Arousal 3 | 26 | / | 2.04 ± 7.90 | 6.48 ± 0.25 | 6.00 ± 6.99 |
| Arousal 4 | 20 | / | 1.57 ± 7.67 | 7.32 ± 0.22 | 7.03 ± 8.16 |

Ratings are expressed as median and its absolute deviation.

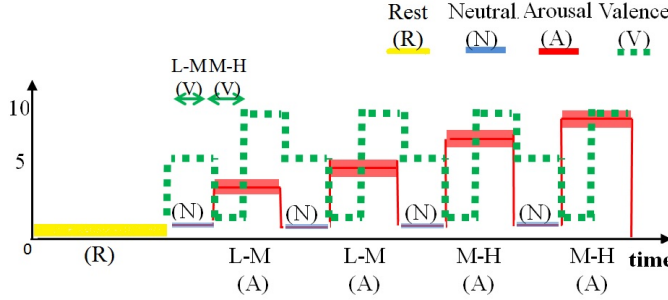


Figure 2: Timeline of the experimental protocol in terms of arousal and valence levels. The vertical axis relates to the IADS score, whereas the horizontal axis relates to the time. The neutral sessions, which are marked with blue lines, alternate with the arousal ones, which are marked with red staircases. Along the time, the red line follows the four arousing sessions having increasing intensity of activation. The dotted green line indicates the valence levels distinguishing the low-medium (L-M) and the medium-high (M-H) level within an arousing session. The neutral sessions are characterized by lowest arousal and medium valence scores. Yellow line relates to the resting state.

2.2 Methodology of Signal Processing

A general block scheme of the whole processing chain is shown in Figure 3. The methodology of signal processing applied to HRV features can be divided into two sections: the extraction of standard and nonlinear features from the HRV series and the Leave One Subject Out Procedure. This procedure applies to the training set through feature selection (statistical analysis) and normalization, whereas to the test set using a trained QDC algorithm. Implementation was performed by using Matlab v8.3.

2.2.1 Standard HRV Measures

Standard HRV analysis refers to the extraction of parameters defined in the time and frequency domain [5], [33], [58].

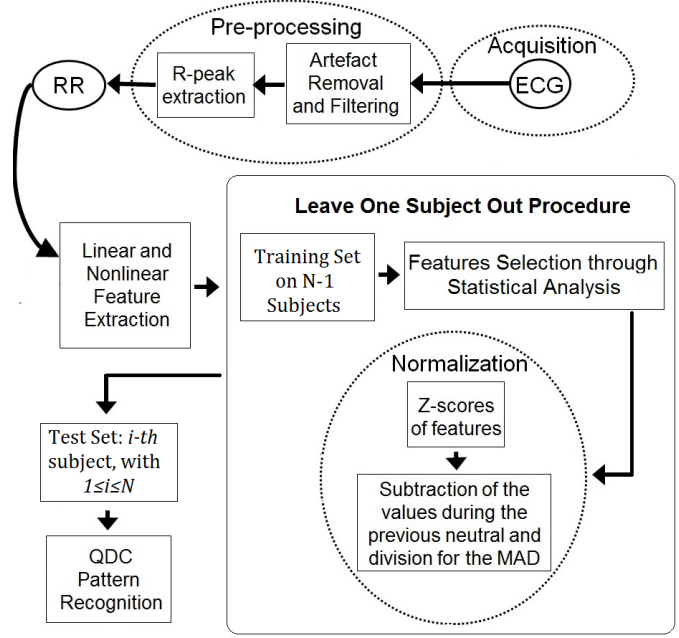


Figure 3: Overall block scheme of the proposed emotion recognition system. The ECG is pre-processed in order to extract the RR interval series. According to the protocol timeline, standard and nonlinear features are extracted and, then, selected through statistical analysis. After a normalization step, QDC algorithms are engaged to perform pattern recognition by adopting a Leave-One-Subject-Out procedure.

Concerning the time domain analysis, we calculated the following features from the HRV series:

- the mean value (RR mean)
- the standard deviation (RR std)
- the standard deviation of NN intervals (the so-called Normal-to-Normal intervals), (SDNN)
- the square root of the mean of the sum of the squares of differences between subsequent NN intervals, ($\text{RMSSD} = \sqrt{\frac{1}{N-1} \sum_{j=1}^{N-1} (RR_{j+1} - RR_j)^2}$)
- the number of successive differences of intervals which differ by more than 50 ms, expressed as a percentage of the total number of heartbeats analyzed ($p\text{NN}50 = \frac{NN50}{N-1} \times 100\%$)
- the integral of the probability density distribution (that is, the number of all NN intervals) divided by the maximum of the probability density distribution, (HRV triangular index, HRV tr. ind.)
- the triangular interpolation of NN interval histogram, that is the baseline width of the distribution measured as a base of a triangle approximating the NN interval distribution (TINN) Between these parameters RMSSD indicates the short term variability, instead SDNN and HRV triangular index are features of the entire HRV [59].

Concerning the frequency domain analysis, several features were calculated from the Power Spectral Density (PSD) analysis. Such a PSD was calculated by using the Welch's

periodogram and window's width and overlap were chosen as a best compromise between the frequency resolution and variance of the estimated spectrum. Three spectral bands of the PSD are identified: VLF (very low frequency) with spectral components below 0.04 Hz; LF (low frequency), ranging between 0.04 and 0.15 Hz; HF (high frequency), comprising frequencies between 0.15 to 0.4 Hz. For each of the three frequency bands these features were computed:

- the power calculated within the VLF, LF, and HF bands.
- the frequencies having maximum magnitude (VLF peak, LF peak, and HF peak).
- the power expressed as percentage of the total power (VLF power %, LF power %, and HF power %).
- the power normalized to the sum of the LF and HF power (LF power nu and HF power nu).
- the LF/HF power ratio.

2.2.2 Nonlinear HRV Measures

From each HRV series, several nonlinear indices were calculated. These measures refer to the estimation and characterization of the phase space (or state space) of the cardiovascular system generating the series. The phase space estimation procedure involves the Takens's method [60], [61] through two parameters: m , the embedding dimension, which is a positive integer, and r , the time delay, which is a positive real number. The parameter m is related to the estimated dimension of the phase space, whereas r is related to the margin of tolerance of the trajectories within the space. Starting from the HRV time series $X = [u(T), u(2T), \dots, u(NT)]$, with T representing the sampling time, attractors of discrete dynamical systems are redefined in a m -dimensional space, operating a delay on the signal. This allows to achieve m signals from only one starting with a lag-time τ :

$$\left\{ \begin{array}{l} X_1 = [u(T), u(2T), \dots, u(mT)] \\ X_2 = [u(2T), u(2T + 2\tau), \dots, u(2T + (m-1)\tau)] \\ \dots \\ X_{N-(m-1)} = [u(N - (m-1))T, \dots, u(N - (m-1))T + (m-1)\tau] \end{array} \right.$$

The vectors x_j are the "delayed coordinates" and the derived m -dimensional space is called "reconstructed space". From the state space theory, several ANS nonlinear parameters can be derived using the following analyses:

From each HRV series, we calculated some nonlinear indices based in particular on three methods: the Approximate Entropy, the Detrended Fluctuation Analysis (DFA) and the Lagged Poincaré Plot (LPP).

- Approximate Entropy

Approximate Entropy is a measure of the unpredictability in the time series. A lower value of ApEn corresponds to a repetitive trend, whereas as higher is the ApEn value as complex is the signal [62], [63].

- Detrended Fluctuation Analysis

The detrended fluctuation analysis features (α_1 and α_2) [64], [65] was evaluated to study correlations on HRV series. Typically, in DFA the correlations are divided into short-term and long-term fluctuations, where the short-term fluctuations of the signal are

characterized by the parameter α_1 and the long-term fluctuations are expressed by α_2 .

- Lagged Poincaré Plots

This technique quantifies the fluctuations of the dynamics of the time series through a graphic (scatter plot of RR intervals) where each RR_n interval is mapped as a function of previous. In this work we also used Lagged Poincaré plot (LPP), a scatter plot of RR_n and RR_{n+M} , with $1 \leq M \leq 10$. The quantitative analysis from the graph can be made by calculating the dispersion of the points in the LPP:

- SD1: the standard deviation related to the points that are perpendicular to the line-of-identity $RR_{n+M} = RR_n$ [43]. It describes the HRV short-term variability.
- SD2: the standard deviation that describes the long-term dynamics and measures the dispersion of the points along the identity line.

Other parameters extracted and analyzed through LPP are as follows:

- SD12 ($SD12 = SD1/SD2$): the ratio between SD1 and SD2. This feature measures the balance between the HRV long and short-term variability [59].
- S ($S = \pi SD1 SD2$): the area of an imaginary ellipse with axes SD1 and SD2 [59], [66].
- SDRR ($SDRR = \frac{1}{\sqrt{2}} \sqrt{SD1^2 + SD2^2}$): an approximate relation indicating the variance of the whole HRV series [66].

2.2.3 Statistical Analysis and Pattern Recognition

Statistical analysis and pattern recognition methodologies were used in this study to automatically recognize the autonomic response on the cardiovascular control of the subjects to the emotional sounds, and to associate the values of the HRV parameters with the kind of elicitation as expressed in terms of arousal and valence. This part of the study has been implemented following the Leave-One-Subject-Out procedure (LOSO): we applied the feature selection and the normalization of the features on a training set made by N-1 subjects (where N is the total number of participants) to recognize the emotional responses of the subject N^{th} . This procedure was iterated N times. The statistical analysis is intended as a preliminary feature selection procedure aimed to select the parameters that significantly vary between the arousal and valence levels, using data gathered from the training set exclusively. Before performing the statistical analysis, Kolmogorov-Smirnov tests were performed in order to check whether the data were normally distributed. In case of non-normal distribution, the results are expressed in terms of median and Median Absolute Deviation ($MAD(X) = Median(|X - Median(X)|)$). Consequently, the Friedman test [67], i.e. nonparametric one-way analysis of variance for paired data, was used to test the null hypothesis that no difference exists among different sessions as well as the Wilcoxon signed-rank test, i.e. a non-parametric statistical hypothesis test used when comparing samples from two sessions, to assess whether their population medians differ. We applied these statistical tests in

order to discern the four arousal sessions, and the negative and positive valence levels of each arousing session.

Every feature, identified as statistically different between sessions, was normalized according to the following steps:

- each feature value extracted from each subject during the neutral session was subtracted from the corresponding value estimated during the successive arousal session;
- each feature value obtained from the previous step was divided by the MAD evaluated over all of the subjects involved in the training set.

Two separate classification algorithms were implemented for the arousal and valence recognition. For each of the two classification algorithms, the dimension of the feature space X , which was chosen as training set, corresponded to the number of selected HRV measures. For the arousal recognition, the number of samples in such a space was related to the number of subjects times the double of the number of arousal sessions (two feature values were extracted for each arousal session), i.e., 26 times 8 equal to 208. The same number of samples was associated to the valence recognition. Finally, both feature sets were used as input of a Quadratic Discriminant Classifier (QDC) [44], [45] which was validated through the Leave-One-Subject-Out (LOSO) procedure [68]. The classification results were expressed as recognition accuracy in form of confusion matrices [69]. A generic element c_{ij} of a confusion matrix indicated the percentage of how many times the feature set belonging to the class i , was recognized as belonging to the class j . This means that a higher average of the values on the matrix diagonal corresponds to a better degree of classification.

Of note, for each of the LOSO steps, the training set was normalized by means of the z-score approach. The mean and standard deviation values of the training set were used to normalize the test sample according to the z-score definition.

3 EXPERIMENTAL RESULTS

All the features described in the previous section were extracted from each HRV series within not overlapped consecutive time windows of one minute and twenty-eight seconds. This length corresponds to the length of each neutral session. Regarding the HRV standard measures, throughout the 27 iterations, significant differences were found on the RRmean, RRstd, RMSSD and TINN. Concerning the HRV features defined in the frequency domain, significant results were found on: LF power %, LF power nu, HF power, HF power %, HF power nu, and LF/HF power ratio. Concerning the HRV nonlinear measures, features as DFA α_1 , DFA α_2 , ApEn, and SD1, SD2, SDRR, and S (extracted by the Poincaré Plots) showed statistically significant differences. This outcome confirmed the importance of the nonlinear analysis in the construction of the emotion recognition classifier, with a special regard to SD12 (see supplementary information for detailed results on the statistical analysis).

An interesting dynamics, shown as a function of the arousal level, is related to the SD12 measure whose plots are reported in Figure 4. Exemplary LPP from a representative

subject are shown in Figure 5. It is clear that the degree of separation between the arousal and corresponding neutral sessions increases according to the degree of the arousing acoustic stimuli.

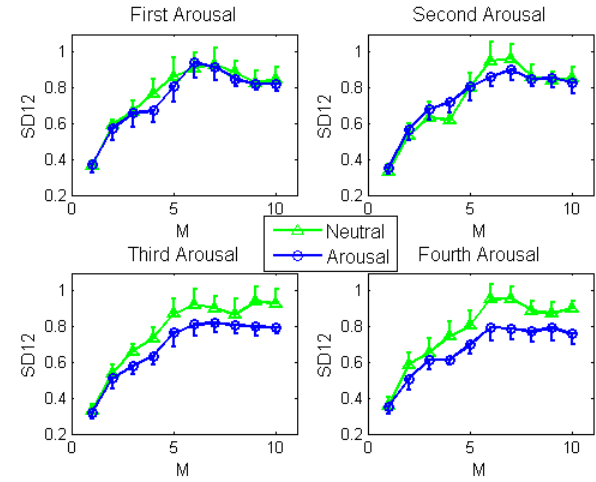


Figure 4: SD12 values as a function of the M lags among the four arousal sessions and corresponding previous neutral sessions.

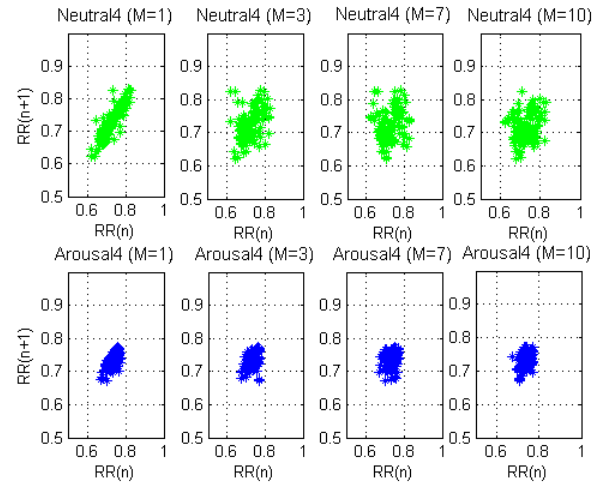


Figure 5: Lagged Poincaré Plots from a representative subject during the elicitation of neutral (top panels) and highest arousing (bottom panels) acoustic stimuli as a function of the M lags.

Every HRV standard and nonlinear measure that showed at least a significant p-value among all the comparisons, both in the arousal and valence dimensions, was included in the feature set constituting the input for the automatic emotion classification through QDC algorithms. Table 2 and 3 report the confusion matrices obtained while discerning the valence and arousal levels, respectively. In particular, table 2 shows the classification accuracy along the valence dimension through which every stimulus is classified regardless of its arousal level. Likewise, table 3 shows the classification accuracy along the arousal dimension through which every stimulus is classified regardless

of its valence level. Of note, neutral stimuli are not taken into account into the automatic classification system because such stimuli are needed for the normalization before the classification (see paragraph 2.2.3). In order to remark the importance of normalization procedure in the proposed algorithm, Table 6 shows the confusion matrix related to the application of the classification algorithm to the non-normalized feature set which, therefore, includes also the neutral session. It is straightforward to note that, in this case, the obtained classification accuracy is not significantly different from random guess (20%).

Table 2: Confusion Matrix of QDC Classifier for Valence Level Recognition

| QDC | Neg.Valence | Pos.Valence |
|-------------|----------------|----------------|
| Neg.Valence | 84.2593 | 14.8148 |
| Pos.Valence | 15.7407 | 85.1852 |

Table 3: Confusion Matrix of QDC Classifier for Arousal Level Recognition

| QDC | Arousal 1 | Arousal 2 | Arousal 3 | Arousal 4 |
|-----------|----------------|----------------|----------------|----------------|
| Arousal 1 | 83.3333 | 14.8148 | 12.9630 | 0 |
| Arousal 2 | 3.7037 | 77.7778 | 5.5556 | 3.7037 |
| Arousal 3 | 11.1111 | 0 | 79.6296 | 0 |
| Arousal 4 | 1.8519 | 7.4074 | 1.8519 | 96.2963 |

In order to study the combined effect of the arousal and valence in the automatic classification system, we developed two further specific arousal classification systems which selectively take unpleasant or pleasant stimuli as an input. Tables 4 and 5 show the classification accuracies, expressed in terms of confusion matrices, while discerning the four arousing levels considering only unpleasant or pleasant acoustic stimuli, respectively.

Table 4: Confusion Matrix of QDC Classifier for Arousal Level Recognition under negative valence

| QDC | Arousal 1 | Arousal 2 | Arousal 3 | Arousal 4 |
|-----------|----------------|----------------|----------------|----------------|
| Arousal 1 | 66.6667 | 51.8519 | 11.1111 | 18.5185 |
| Arousal 2 | 11.1111 | 25.9259 | 22.2222 | 3.7037 |
| Arousal 3 | 11.1111 | 11.1111 | 51.8518 | 18.5185 |
| Arousal 4 | 11.1111 | 11.1111 | 14.8148 | 59.2593 |

Table 5: Confusion Matrix of QDC Classifier for Arousal Level Recognition under positive valence

| QDC | Arousal 1 | Arousal 2 | Arousal 3 | Arousal 4 |
|-----------|----------------|----------------|----------------|----------------|
| Arousal 1 | 59.2593 | 37.0370 | 29.6296 | 37.0370 |
| Arousal 2 | 25.9259 | 55.5556 | 33.3333 | 18.5185 |
| Arousal 3 | 0 | 3.7037 | 22.2222 | 7.4074 |
| Arousal 4 | 14.8148 | 3.7037 | 14.8148 | 37.0370 |

4 CONCLUSION AND DISCUSSION

In conclusion, in this study we presented a novel approach to automatically recognize emotions, as elicited by affective sounds, in young healthy subjects through the analysis of the cardiovascular dynamics exclusively. Emotions are expressed in terms of arousal and valence levels according

Table 6: Confusion Matrix of QDC Classifier for Arousal Level Recognition without normalization

| QDC | Arous1 | Arous2 | Arous3 | Arous4 | Neutral |
|----------|----------------|----------------|----------------|---------------|---------------|
| Arousal1 | 14,8148 | 11,1111 | 18,5185 | 7,4074 | 11,1111 |
| Arousal2 | 37,0370 | 18,5185 | 25,9259 | 29,6296 | 40,7407 |
| Arousal3 | 33,3333 | 44,4444 | 18,5185 | 33,3333 | 29,6296 |
| Arousal4 | 11,1111 | 14,8148 | 11,1111 | 7,4074 | 11,1111 |
| Neutral | 3,7037 | 11,1111 | 25,9259 | 22,2222 | 7,4074 |

to the Russel's circumplex model of affect [2], whereas the cardiovascular dynamics is estimated through standard and nonlinear HRV measures, which have been demonstrated to be effective quantifiers of the ANS activity on the cardiovascular control. The experimental results showed a recognition accuracy of 84.72% on the valence dimension, and 84.26% on the arousal dimension. This study also suggested that ANS measures such as the HRV mean value, std, RMSSD, triangular index, spectral measures, and standard deviations of the LPP are the most effective HRV features to recognize emotional states induced by affective sounds.

Specifically, the automatic classification system is built on the subject's physiological response, which is quantified through standard and nonlinear HRV measures. These features were selected according to their discerning capabilities among the sessions of elicitation. A relevant contribution was given by nonlinear parameters of defined by LPP. This finding confirms the relevant contribution of nonlinear analysis in the affective computing field, especially in the analysis of cardiac signals [5], [43], [70]. Moreover, this result is in agreement with the current literature showing the crucial role of LPP analysis during acoustic elicitation [70]–[74]. Among the other LPP measures, the SD1 measures, which represents the instantaneous beat-to-beat variability of RR intervals, and SD12, which represents the ratio between the two standard deviations, have been associated to the parasympathetic activity [43], [75], [76]. Thus, a decrease of these indices could be associated to a corresponding reduction of the parasympathetic modulation. A clear decrease of the SD1 measure is shown in Figure 5, revealing differences between the highest arousing session and corresponding neutral session in a representative subject. The shape of the Poincaré plots on the neutral session becomes more circular along the lag increase, while the plots corresponding to the arousing session are elliptically shaped. This implies significant changes in the ANS dynamical response to standardized emotional elicitation through sounds. Of note, these results are in agreement with previous studies describing ANS changes during meditation [77]. We found a decrease of these features going from neutral to arousing stimuli, and from negative to positive sounds. These changes are also confirmed by other measures such as RMSSD and pNN50 defined in the time domain, and measures such as HF defined in the frequency domain [75]. Concerning the entropy measures, ApEn significantly contributed in discerning auditory affective elicitations, broadening its crucial role in an emotion recognition system previously highlighted for affective images [5], [35], [78].

As mentioned above, the results of the classification, validated through LOSO approach, were very satisfactory. We used the QDC because of its effectiveness in dealing

with multivariate input space and its wide use in other clinical studies [5], [79], [80]. Note that other classification algorithms such as Linear Discriminant Classifier, k-Nearest Neighbor, Kohonen Self Organizing map, and Multilayer Perceptron were tested in this study. Among these, QDC showed the highest recognition accuracy in both arousal and valence classification.

The normalization of the feature values, performed by subtracting the values from the previous neutral session, was carried out in order to evaluate the deviations of the features in arousal and valence sessions from the corresponding neutral ones. The normalization procedure improved the classification accuracy. Indeed, performing the arousal and valence classification through the implementation of the same processing chain described in paragraph 2.2 without the normalization procedure, we obtained poor classification performances (**Table 6**). Of note, we also proposed a valence-specific classification system for the arousal levels. The recognition accuracy associated to the arousal level 1 and arousal level 4 is much higher than the ones associated to the arousal level 2 and arousal level 3. Note that the experimental protocol foresaw elicitation sessions alternating neutral and arousing sessions, and valence sessions are embedded within each arousing session. In order to comply with the minimum signal-length requirement for the computation of the HRV features, we were able to properly identify two valence levels (unpleasant/negative and pleasant/positive) within each arousing session. Each valence interval, in fact, lasted for 1.28 minutes. To our knowledge, this study shows for the first time the use of autonomic nervous system measures, as estimated in the time/frequency/nonlinear domain, to recognize emotional states induced by affective sounds. It is also worthwhile noting that we were able to discern pleasant and unpleasant, and arousing stimuli by using features extracted from the HRV series exclusively. The achievement of this challenging task opens new avenues in the field of affective computing, suggesting that emotion recognition is possible using data coming from ECG only. Emotion recognition through ECG only was already performed in the literature [37], [81], [82]. However, to our knowledge, the use of the IADS database in emotion recognition using ECG only is a great novelty in the current literature. Other novelties of this work include the use of LPP for the analysis of the ANS dynamics. This research can have a high impact in the field of affective computing because it will be possible to use the proposed system in naturalistic applications involving wearable monitoring systems such as simple holter ECG or smart textiles [10].

This study also confirms that the analysis of peripheral physiological measures allows to differentiate emotions because of the modulation of the ANS dynamics on the cardiovascular control by important areas in the central nervous system [53], [83]–[86]. In particular, the prefrontal cortex, the lateral hypothalamus, the cingulate anterior cortex, amygdala are known to modulate the activity of the nucleus of the solitary tract and the nucleus ambiguus which, together, modulate the sympathetic and parasympathetic efferent ways to the heart whose variability dynamics is detected by the system proposed in this work. At the same time, the central nucleus of amygdala is known to

be directly involved in the regulation of autonomic and neuroendocrine responses in situations with a high level of emotional stimulations [87]. Indeed, changes observed during such a stimulation in the parameters extracted from HRV reflect changes in ANS dynamics particularly related to the parasympathetic nervous system, thus confirming the importance of the vagus nerve in the communication between the Central Nervous System and the heart during emotion regulation [81], [88].

ACKNOWLEDGEMENT

The authors are grateful to Riccardo Crupi for helping during the experimental set-up, data acquisition, and recruitment of eligible subjects.

REFERENCES

- [1] R. W. Picard, "Affective computing: challenges," *International Journal of Human-Computer Studies*, vol. 59, no. 1, pp. 55–64, 2003.
- [2] J. A. Russell, "A circumplex model of affect," *Journal of personality and social psychology*, vol. 39, no. 6, p. 1161, 1980.
- [3] J. Posner, J. A. Russell, and B. S. Peterson, "The circumplex model of affect: An integrative approach to affective neuroscience, cognitive development, and psychopathology," *Development and psychopathology*, vol. 17, no. 03, pp. 715–734, 2005.
- [4] G. Valenza, A. Lanata, and E. P. Scilingo, "Oscillations of heart rate and respiration synchronize during affective visual stimulation," *Information Technology in Biomedicine, IEEE Transactions on*, vol. 16, no. 4, pp. 683–690, 2012.
- [5] ———, "The role of nonlinear dynamics in affective valence and arousal recognition," *Affective Computing, IEEE Transactions On*, vol. 3, no. 2, pp. 237–249, 2012.
- [6] R. W. Levenson, "Emotion and the autonomic nervous system: A prospectus for research on autonomic specificity," *Social psychophysiology and emotion: Theory and clinical applications*, pp. 17–42, 1988.
- [7] G. Valenza, M. Nardelli, A. Lanata, C. Gentili, G. Bertschy, R. Paradiso, and E. P. Scilingo, "Wearable monitoring for mood recognition in bipolar disorder based on history-dependent long-term heart rate variability analysis," *IEEE Journal of Biomedical and Health Informatics*, vol. 18, no. 5, 2014.
- [8] J. L. Andreassi, *Psychophysiology: Human behavior and physiological response*. Psychology Press, 2000.
- [9] K. H. Kim, S. Bang, and S. Kim, "Emotion recognition system using short-term monitoring of physiological signals," *Medical and biological engineering and computing*, vol. 42, no. 3, pp. 419–427, 2004.
- [10] A. Lanata, G. Valenza, and E. P. Scilingo, "A novel eda glove based on textile-integrated electrodes for affective computing," *Medical & biological engineering & computing*, vol. 50, no. 11, pp. 1163–1172, 2012.
- [11] T. Partala and V. Surakka, "Pupil size variation as an indication of affective processing," *International journal of human-computer studies*, vol. 59, no. 1, pp. 185–198, 2003.
- [12] A. Lanata, A. Armato, G. Valenza, and E. P. Scilingo, "Eye tracking and pupil size variation as response to affective stimuli: a preliminary study," in *Pervasive Computing Technologies for Healthcare (PervasiveHealth), 2011 5th International Conference on*. IEEE, 2011, pp. 78–84.
- [13] W. Boucsein, *Electrodermal activity*. Springer, 2012.
- [14] J. Wagner, J. Kim, and E. André, "From physiological signals to emotions: Implementing and comparing selected methods for feature extraction and classification," in *Multimedia and Expo, 2005. ICME 2005. IEEE International Conference on*. IEEE, 2005, pp. 940–943.
- [15] G. Valenza, A. Lanata, E. P. Scilingo, and D. De Rossi, "Towards a smart glove: Arousal recognition based on textile electrodermal response," in *Engineering in Medicine and Biology Society (EMBC), 2010 Annual International Conference of the IEEE*. IEEE, 2010, pp. 3598–3601.

- [16] F. Nasoz, K. Alvarez, C. L. Lisetti, and N. Finkelstein, "Emotion recognition from physiological signals using wireless sensors for presence technologies," *Cognition, Technology & Work*, vol. 6, no. 1, pp. 4–14, 2004.
- [17] F. Nasoz, C. L. Lisetti, K. Alvarez, and N. Finkelstein, "Emotion recognition from physiological signals for user modeling of affect," in *Proceedings of the 3rd Workshop on Affective and Attitude User Modelling (Pittsburgh, PA, USA)*, 2003.
- [18] A. Greco, G. Valenza, A. Lanata, G. Rota, and E. P. Scilingo, "Electrodermal activity in bipolar patients during affective elicitation," *IEEE Journal of Biomedical and Health Informatics*, 2014.
- [19] J. A. Healey, "Affect detection in the real world: Recording and processing physiological signals," in *Affective Computing and Intelligent Interaction and Workshops, 2009. ACII 2009. 3rd International Conference on*. IEEE, 2009, pp. 1–6.
- [20] J. Rottenberg, R. D. Ray, and J. J. Gross, "Emotion elicitation using films," 2007.
- [21] J. J. Gross and R. W. Levenson, "Emotion elicitation using films," *Cognition & Emotion*, vol. 9, no. 1, pp. 87–108, 1995.
- [22] L. Li and J.-h. Chen, "Emotion recognition using physiological signals," in *Advances in Artificial Reality and Tele-Existence*. Springer, 2006, pp. 437–446.
- [23] A. Pechinenda, "The affective significance of skin conductance activity during a difficult problem-solving task," *Cognition & Emotion*, vol. 10, no. 5, pp. 481–504, 1996.
- [24] J. Scheirer, R. Fernandez, J. Klein, and R. W. Picard, "Frustrating the user on purpose: a step toward building an affective computer," *Interacting with computers*, vol. 14, no. 2, pp. 93–118, 2002.
- [25] A. Greco, A. Lanata, G. Valenza, G. Rota, N. Vanello, and E. Scilingo, "On the deconvolution analysis of electrodermal activity in bipolar patients," in *Engineering in Medicine and Biology Society (EMBC), 2012 Annual International Conference of the IEEE*. IEEE, 2012, pp. 6691–6694.
- [26] M. Ilves and V. Surakka, "Heart rate responses to synthesized affective spoken words," *Advances in Human-Computer Interaction*, vol. 2012, p. 14, 2012.
- [27] Y.-H. Yang and H. H. Chen, *Music Emotion Recognition*. CRC Press, 2011.
- [28] Y.-H. Yang, Y.-C. Lin, Y.-F. Su, and H. H. Chen, "A regression approach to music emotion recognition," *Audio, Speech, and Language Processing, IEEE Transactions on*, vol. 16, no. 2, pp. 448–457, 2008.
- [29] J. Kim and E. André, "Emotion recognition based on physiological changes in music listening," *Pattern Analysis and Machine Intelligence, IEEE Transactions on*, vol. 30, no. 12, pp. 2067–2083, 2008.
- [30] M. M. Bradley and P. J. Lang, "The international affective digitized sounds (iads-2): Affective ratings of sounds and instruction manual," *University of Florida, Gainesville, FL, Tech. Rep. B-3*, 2007.
- [31] P. J. Lang, M. M. Bradley, B. N. Cuthbert et al., *International affective picture system (IAPS): Affective ratings of pictures and instruction manual*. NIMH, Center for the Study of Emotion & Attention, 2005.
- [32] P. J. Lang, M. M. Bradley, and B. N. Cuthbert, "International affective picture system (iaps): Technical manual and affective ratings," 1999.
- [33] A. Camm, M. Malik, J. Bigger, G. Breithardt, S. Cerutti, R. Cohen et al., "Heart rate variability: standards of measurement, physiological interpretation, and clinical use," *Circulation*, vol. 93, no. 5, pp. 1043–1065, 1996.
- [34] K. Sunagawa, T. Kawada, and T. Nakahara, "Dynamic nonlinear vago-sympathetic interaction in regulating heart rate," *Heart and vessels*, vol. 13, no. 4, pp. 157–174, 1998.
- [35] G. Valenza, P. Allegrini, A. Lanatà, and E. P. Scilingo, "Dominant lyapunov exponent and approximate entropy in heart rate variability during emotional visual elicitation," *Frontiers in neuroengineering*, vol. 5, 2012.
- [36] G. Valenza, M. Nardelli, G. Bertschy, A. Lanata, and E. Scilingo, "Mood states modulate complexity in heartbeat dynamics: A multiscale entropy analysis," *EPL (Europhysics Letters)*, vol. 107, no. 1, p. 18003, 2014.
- [37] G. Valenza, L. Citi, A. Lanatà, E. P. Scilingo, and R. Barbieri, "Revealing real-time emotional responses: a personalized assessment based on heartbeat dynamics," *Scientific reports*, vol. 4, 2014.
- [38] G. Valenza, L. Citi, A. Lanata, E. Scilingo, and R. Barbieri, "A nonlinear heartbeat dynamics model approach for personalized emotion recognition," in *Engineering in Medicine and Biology Society (EMBC), 2013 35th Annual International Conference of the IEEE*. IEEE, 2013, pp. 2579–2582.
- [39] G. Valenza, L. Citi, and R. Barbieri, "Estimation of instantaneous complex dynamics through lyapunov exponents: a study on heart-beat dynamics," *PloS one*, vol. 9, no. 8, p. e105622, 2014.
- [40] G. Valenza, L. Citi, C. Gentili, A. Lanatà, E. Scilingo, and R. Barbieri, "Characterization of depressive states in bipolar patients using wearable textile technology and instantaneous heart rate variability assessment," *IEEE Journal of Biomedical and Health Informatics*, 2014.
- [41] A. L. Roque, V. E. Valenti, H. L. Guida, M. F. Campos, A. Knap, L. C. M. Vanderlei, L. L. Ferreira, C. Ferreira, and L. C. de Abreu, "The effects of auditory stimulation with music on heart rate variability in healthy women," *Clinics*, vol. 68, no. 7, pp. 960–967, 2013.
- [42] S. A. F. da Silva, H. L. Guida, A. M. dos SantosAntônio, L. C. M. Vanderlei, L. L. Ferreira, L. C. de Abreu, F. H. Sousa, and V. E. Valenti, "Auditory stimulation with music influences the geometric indices of heart rate variability in men," *International Archives of Medicine*, vol. 7, no. 1, pp. 1–7, 2014.
- [43] B. Roy, R. Choudhuri, A. Pandey, S. Bandopadhyay, S. Sarangi, and S. K. Ghatak, "Effect of rotating acoustic stimulus on heart rate variability in healthy adults," *The open neurology journal*, vol. 6, p. 71, 2012.
- [44] H. Duda, P. Hart et al., "Stork, pattern classification," 2001.
- [45] S. Srivastava, M. R. Gupta, and B. A. Frigyiak, "Bayesian quadratic discriminant analysis," *Journal of Machine Learning Research*, vol. 8, no. 6, pp. 1277–1305, 2007.
- [46] J. Anttonen and V. Surakka, "Emotions and heart rate while sitting on a chair," in *Proceedings of the SIGCHI conference on Human factors in computing systems*. ACM, 2005, pp. 491–499.
- [47] L. Ivonin, H.-M. Chang, W. Chen, and M. Rautenberg, "Unconscious emotions: quantifying and logging something we are not aware of," *Personal and ubiquitous computing*, vol. 17, no. 4, pp. 663–673, 2013.
- [48] M. M. Bradley and P. J. Lang, "Affective reactions to acoustic stimuli," *Psychophysiology*, vol. 37, no. 02, pp. 204–215, 2000.
- [49] C. Martin-Soelch, M. Stöcklin, G. Dammann, K. Opwis, and E. Seifritz, "Anxiety trait modulates psychophysiological reactions, but not habituation processes related to affective auditory stimuli," *International journal of psychophysiology*, vol. 61, no. 2, pp. 87–97, 2006.
- [50] A. Keil, M. M. Bradley, M. Junghöfer, T. Russmann, W. Lowenthal, and P. J. Lang, "Cross-modal attention capture by affective stimuli: evidence from event-related potentials," *Cognitive, Affective, & Behavioral Neuroscience*, vol. 7, no. 1, pp. 18–24, 2007.
- [51] Y.-P. Lin, C.-H. Wang, T.-P. Jung, T.-L. Wu, S.-K. Jeng, J.-R. Duann, and J.-H. Chen, "Eeg-based emotion recognition in music listening," *Biomedical Engineering, IEEE Transactions on*, vol. 57, no. 7, pp. 1798–1806, 2010.
- [52] M. Orini, R. Bailón, R. Enk, S. Koelsch, L. Mainardi, and P. Laguna, "A method for continuously assessing the autonomic response to music-induced emotions through hrv analysis," *Medical & biological engineering & computing*, vol. 48, no. 5, pp. 423–433, 2010.
- [53] S. Anders, F. Eippert, N. Weiskopf, and R. Veit, "The human amygdala is sensitive to the valence of pictures and sounds irrespective of arousal: an fmri study," *Social cognitive and affective neuroscience*, vol. 3, no. 3, pp. 233–243, 2008.
- [54] J. Pan and W. J. Tompkins, "A real-time qrs detection algorithm," *Biomedical Engineering, IEEE Transactions on*, no. 3, pp. 230–236, 1985.
- [55] N. Lippman, K. Stein, and B. Lerman, "Comparison of methods for removal of ectopy in measurement of heart rate variability," *American Journal of Physiology-Heart and Circulatory Physiology*, vol. 267, no. 1, p. H411, 1994.
- [56] G. Berntson et al., "Heart rate variability: origins, methods, and interpretive caveats," *Psychophysiology*, vol. 34, no. 6, pp. 623–648, 1997.
- [57] M. Tarvainen, P. Ranta-Aho, and P. Karjalainen, "An advanced detrending method with application to hrv analysis," *Biomedical Engineering, IEEE Transactions on*, vol. 49, no. 2, pp. 172–175, 2002.
- [58] U. R. Acharya, K. P. Joseph, N. Kannathal, C. M. Lim, and J. S. Suri, "Heart rate variability: a review," *Medical and Biological Engineering and Computing*, vol. 44, no. 12, pp. 1031–1051, 2006.
- [59] P. Guzik, J. Piskorski, T. Krauze, R. Schneider, K. H. Wesseling, A. Wykretowicz, and H. Wysocki, "Correlations between the poincare plot and conventional heart rate variability parameters assessed during paced breathing," *The Journal of Physiological Sciences*, vol. 57, no. 1, pp. 63–71, 2007.

- [60] F. Takens, "Detecting strange attractors in turbulence," in *Dynamical systems and turbulence, Warwick 1980*. Springer, 1981, pp. 366–381.
- [61] M. Casdagli, S. Eubank, J. D. Farmer, and J. Gibson, "State space reconstruction in the presence of noise," *Physica D: Nonlinear Phenomena*, vol. 51, no. 1, pp. 52–98, 1991.
- [62] Y. Fusheng, H. Bo, and T. Qingyu, "Approximate entropy and its application to biosignal analysis," *Nonlinear Biomedical Signal Processing: Dynamic Analysis and Modeling, Volume 2*, pp. 72–91, 2001.
- [63] S. M. Pincus, "Approximate entropy as a measure of system complexity," *Proceedings of the National Academy of Sciences*, vol. 88, no. 6, pp. 2297–2301, 1991.
- [64] C.-K. Peng, S. Havlin, H. E. Stanley, and A. L. Goldberger, "Quantification of scaling exponents and crossover phenomena in nonstationary heartbeat time series," *Chaos: An Interdisciplinary Journal of Nonlinear Science*, vol. 5, no. 1, pp. 82–87, 1995.
- [65] T. Penzel, J. W. Kantelhardt, L. Grote, J.-H. Peter, and A. Bunde, "Comparison of detrended fluctuation analysis and spectral analysis for heart rate variability in sleep and sleep apnea," *Biomedical Engineering, IEEE Transactions on*, vol. 50, no. 10, pp. 1143–1151, 2003.
- [66] J. Piskorski and P. Guzik, "Filtering poincare plots," *Computational methods in science and technology*, vol. 11, no. 1, pp. 39–48, 2005.
- [67] J. D. Gibbons and S. Chakraborti, *Nonparametric statistical inference*. Springer, 2011.
- [68] M. Kearns and D. Ron, "Algorithmic stability and sanity-check bounds for leave-one-out cross-validation," *Neural Computation*, vol. 11, no. 6, pp. 1427–1453, 1999.
- [69] R. Kohavi and F. Provost, "Glossary of terms," *Machine Learning*, vol. 30, no. 2-3, pp. 271–274, 1998.
- [70] P. Shi, Y. Zhu, J. Allen, and S. Hu, "Analysis of pulse rate variability derived from photoplethysmography with the combination of lagged poincaré plots and spectral characteristics," *Medical engineering & physics*, vol. 31, no. 7, pp. 866–871, 2009.
- [71] M. Malik, J. T. Bigger, A. J. Camm, R. E. Kleiger, A. Malliani, A. J. Moss, and P. J. Schwartz, "Heart rate variability standards of measurement, physiological interpretation, and clinical use," *European heart journal*, vol. 17, no. 3, pp. 354–381, 1996.
- [72] M. Brennan, M. Palaniswami, and P. Kamen, "Do existing measures of poincare plot geometry reflect nonlinear features of heart rate variability?" *Biomedical Engineering, IEEE Transactions on*, vol. 48, no. 11, pp. 1342–1347, 2001.
- [73] ———, "Poincaré plot interpretation using a physiological model of hrv based on a network of oscillators," *American Journal of Physiology-Heart and Circulatory Physiology*, vol. 283, no. 5, pp. H1873–H1886, 2002.
- [74] R. A. Hoshi, C. M. Pastre, L. C. M. Vanderlei, and M. F. Godoy, "Poincaré plot indexes of heart rate variability: Relationships with other nonlinear variables," *Autonomic Neuroscience*, vol. 177, no. 2, pp. 271–274, 2013.
- [75] L. Mourot, M. Bouhaddi, S. Perrey, S. Cappelle, M.-T. Henriet, J.-P. Wolf, J.-D. Rouillon, and J. Regnard, "Decrease in heart rate variability with overtraining: assessment by the poincaré plot analysis," *Clinical physiology and functional imaging*, vol. 24, no. 1, pp. 10–18, 2004.
- [76] P. W. Kamen, H. Krum, and A. M. Tonkin, "Poincare plot of heart rate variability allows quantitative display of parasympathetic nervous activity in humans," *Clinical science*, vol. 91, no. 2, pp. 201–208, 1996.
- [77] A. Goshvarpour, A. Goshvarpour, and S. Rahati, "Analysis of lagged poincare plots in heart rate signals during meditation," *Digital Signal Processing*, vol. 21, no. 2, pp. 208–214, 2011.
- [78] G. Valenza, L. Citi, E. P. Scilingo, and R. Barbieri, "Inhomogeneous point-process entropy: An instantaneous measure of complexity in discrete systems," *Physical Review E*, vol. 89, no. 5, p. 052803, 2014.
- [79] R. S. Ryback, M. J. Eckardt, R. R. Rawlings, and L. S. Rosenthal, "Quadratic discriminant analysis as an aid to interpretive reporting of clinical laboratory tests," *Jama*, vol. 248, no. 18, pp. 2342–2345, 1982.
- [80] G. Valenza, A. Lanatá, and E. P. Scilingo, "Improving emotion recognition systems by embedding cardiorespiratory coupling," *Physiological measurement*, vol. 34, no. 4, p. 449, 2013.
- [81] R. D. Lane, K. McRae, E. M. Reiman, K. Chen, G. L. Ahern, and J. F. Thayer, "Neural correlates of heart rate variability during emotion," *Neuroimage*, vol. 44, no. 1, pp. 213–222, 2009.
- [82] B. M. Appelhans and L. J. Luecken, "Heart rate variability as an index of regulated emotional responding," *Review of general psychology*, vol. 10, no. 3, p. 229, 2006.
- [83] J. Iwata, K. Chida, and J. E. LeDoux, "Cardiovascular responses elicited by stimulation of neurons in the central amygdaloid nucleus in awake but not anesthetized rats resemble conditioned emotional responses," *Brain research*, vol. 418, no. 1, pp. 183–188, 1987.
- [84] D. Palomba, A. Angrilli, and A. Mini, "Visual evoked potentials, heart rate responses and memory to emotional pictorial stimuli," *International Journal of Psychophysiology*, vol. 27, no. 1, pp. 55–67, 1997.
- [85] J. M. Hitchcock and M. Davis, "Efferent pathway of the amygdala involved in conditioned fear as measured with the fear-potentiated startle paradigm," *Behavioral neuroscience*, vol. 105, no. 6, p. 826, 1991.
- [86] G. Valenza, L. Citi, C. Gentili, A. Lanatá, E. Scilingo, and R. Barbieri, "Point-process nonlinear autonomic assessment of depressive states in bipolar patients," *Methods of Information in Medicine*, 2014.
- [87] A. Wiersma, B. Bohus, and J. Koolhaas, "Corticotropin-releasing hormone microinfusion in the central amygdala diminishes a cardiac parasympathetic outflow under stress-free conditions," *Brain research*, vol. 625, no. 2, pp. 219–227, 1993.
- [88] S. W. Porges, J. A. Doussard-Roosevelt, and A. K. Maiti, "Vagal tone and the physiological regulation of emotion," *Monographs of the Society for Research in Child Development*, vol. 59, no. 2-3, pp. 167–186, 1994.